Neuroinformatics

ISSN 1539-2791/04/145–162/$25.00

Review Article

The Small World of the Cerebral Cortex

Olaf Sporns[*] *and Jonathan D. Zwi*

Department of Psychology, Indiana University, Bloomington, IN 47405

Abstract

While much information is available on the structural connectivity of the cerebral cortex, especially in the primate, the main organizational principles of the connection patterns linking brain areas, columns and individual cells have remained elusive. We attempt to characterize a wide variety of cortical connectivity data sets using a specific set of graph theory methods. We measure global aspects of cortical graphs including the abundance of small structural motifs such as cycles, the degree of local clustering of connections and the average path length. We examine large-scale cortical connection matrices obtained from neuroanatomical data bases, as well as probabilistic connection matrices at the level of small cortical neuronal populations linked by intra-areal and inter-areal connections. All cortical connection matrices examined in this study exhibit "small-world" attributes, characterized by the presence of abundant clustering of connections combined with short average distances between neuronal elements. We discuss the significance of these universal organizational features of cortex in light of functional brain anatomy. Supplementary materials are at www.indiana.edu/~cortex/lab.htm.

Index Entries: Network; computational neuroanatomy; small world; complexity; information.

Introduction

The human cerebral cortex consists of approx 10^{11} neurons linked by 10^{15} connections, forming a complex network that is extremely sparse, yet capable of integrated real-time performance. To better understand the functioning of the human brain, we need a comprehensive structural model of its architecture. A broad range of anatomical and physiological studies have revealed at least some basic features of cortical connectivity. A large proportion of intra-cortical connections are made locally, linking neurons that are separated by only a

[*]Address to which all correspondence and reprint requests should be sent.
E-mail: osporns@indiana.edu

few hundred micrometers (Nicoll and Blakemore, 1993; Liley and Wright, 1994) and often share similar response properties. Another large proportion of connections extends over longer distances, linking neurons that are located in different cortical regions. These connections, forming large-scale networks of interregional pathways, ensure that distant cortical sites can interact rapidly, usually within tens or hundreds of milliseconds, to generate dynamical patterns of temporal correlations (Bressler, 1995; Varela et al., 2001). Thus, it appears that cortical connectivity plays a dual role in neural processing. First, it is critical in generating functional specificity (i.e., information) of local cell populations and areas within cortex. Second, it allows the integration of different sources of information into coherent behavioral and cognitive states.

A resurgence of interest in network structure and dynamics was sparked by the discovery of a class of networks that combines densely clustered connectivity with a small admixture of random connections. Such networks combine structural features of completely random and completely regular connection topologies. They preserve a high degree of connectivity within local neighborhoods while allowing all nodes of the network to be linked by surprisingly short paths, creating a "small world" within the network. Small-world networks are ubiquitous in natural, social and technological systems (Milgram, 1967; Watts and Strogatz, 1998; Jeong et al., 1999; Albert et al., 1999; Strogatz, 2001; Albert and Barabasi, 2002; Barabasi, 2002; Watts, 2003). Their comparative analysis is based on a representation of networks as graphs (e.g., Harary, 1969; Chartrand and Lesniak, 1996), consisting of a set of vertices (units) linked by a set of edges (connections). Graphs represent the topology of a network and usually discount its physical metric realization.

A major motivation behind attempts to quantify and measure global aspects of network organization is the recognized importance of network structure and topology for the functioning and dynamics of integrated systems. Nervous systems are no exception. The topology of neural connectivity critically affects the spread of neural signals and of neural information. Despite its importance for neural information processing, the topology of cortical networks is still only partially understood. We still have only rudimentary and extremely sketchy information on the connection matrix of the brain of any species (Bota et al., 2003), especially that of the human cortex (Crick and Jones, 1993). Most complete information is available for large-scale cortico-cortical pathways in various mammalian species, which have been catalogued in several comprehensive surveys (Felleman and van Essen, 1991; Young, 1993; Scannell and Young, 1993; Scannell et al., 1995, 1999) and are increasingly available in online databases (Kötter, 2001), including Cocomac (2003), BAMS (2003), and the USC Brain Project (2003). In addition, there is a wealth of empirical data from neuroanatomical and electrophysiological studies on the patterning of cortico-cortical connections linking neurons within and between brain regions (e.g., Liley and Wright, 1994; Braitenberg and Schüz, 1998; Hellwig, 2000). The increasing volume of connectional information necessitates the development of new methods for computational neuroanatomy (Ascoli, 2002), including ways to collect, store, and archive connection data sets.

In this paper, we structurally analyze a set of large-scale cortical connectivity datasets, with special emphasis on global measures of network organization. Neuronal connectivity patterns are represented as directed graphs with vertices (brain areas or neurons) that are connected by directed edges (synapses or connections). We utilize a set of graph theoretical tools (Sporns et al., 2000; Sporns, 2002) to quantify the structural characteristics of large-scale cortical networks. We extend this analysis

to other cortical connections patterns that incorporate information on the density of corticocortical pathways. We also generate connection patterns based on measurements of statistical connection probability between neurons separated by some metric distance. In all cases, we find that cortical connection patterns exhibit small-world properties, characterized by the simultaneous existence of short paths between all constituent elements and of a high degree of clustering.

Methods

Large-Scale Connectivity Data Sets

All large-scale connectivity data sets analyzed in this paper are binary connection matrices obtained from published reviews or from neuroinformatics databases. The corresponding graphs consist of N brain areas (vertices) linked by K connection pathways (directed edges). In all cases, an entry $c_{ij} = 1$ represents the presence of a pathway from element *j* to element *i*, while an entry $c_{ij} = 0$ represents the confirmed absence of such a pathway, or represents pathways whose existence has not yet been experimentally verified. In all cases, all $c_{ii} = 0$. In this article, we do not provide complete listings of abbreviations for the names of brain regions, but rather, direct the reader to the original publications.

Macaque Visual Cortex

The connection matrix (Fig. 1A) is based on the original publication by Felleman and van Essen (1991), and was modified as follows: The connections of areas {PITd, PIT, PITv}, {CITd, CIT, CITv}, and {STPp, STP, STPa} were consolidated by eliminating PIT, CIT, and STP and assigning their connections to {PITd, PITv}, {CITd, CITv}, and {STPp, STPa}, respectively. Areas MIP and MDP were eliminated because of lack of connectional information. The modified matrix has N = 30 and K = 311.

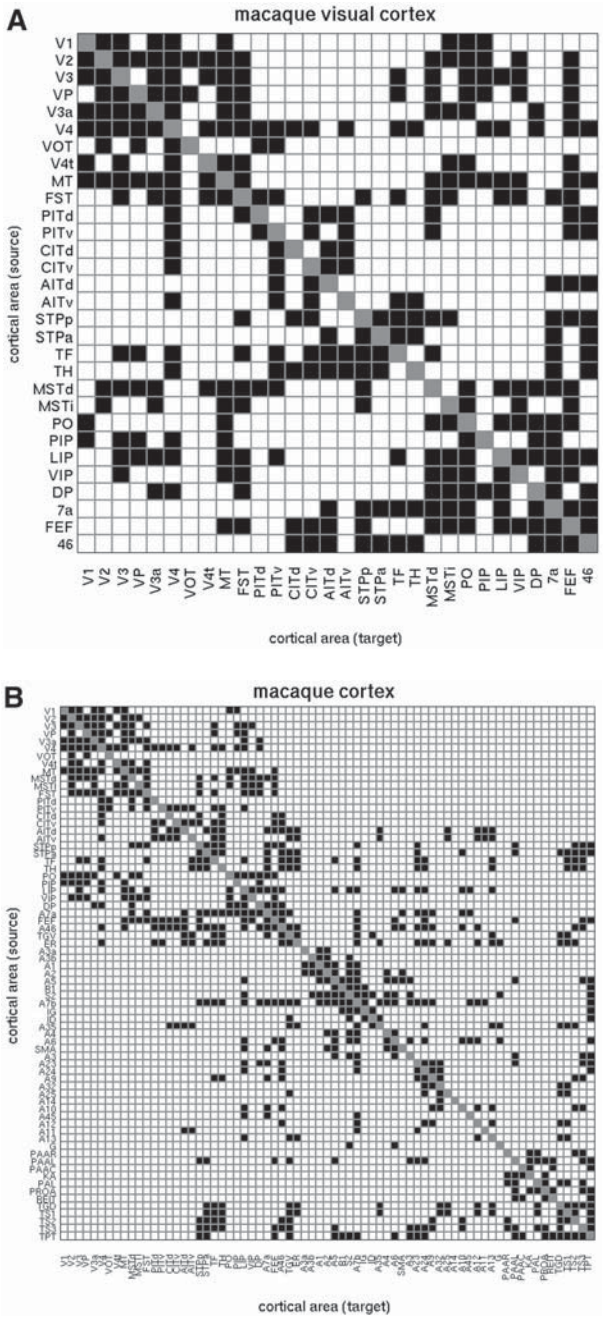

Fig. 1. (*Continued on next page*)

Macaque Cortex

The connection matrix (Fig. 1B) is based on the paper by Young (1993) and was kindly provided by Claus Hilgetag (IU Bremen). Two areas, HIPP (hippocampus) and AMYG (amygdala)

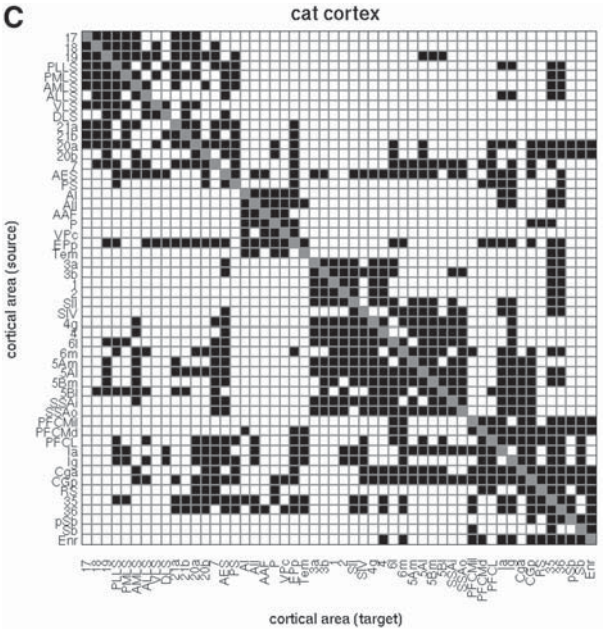

Fig. 1. Large-scale connection matrices used in the paper. White entries denote c_{ij} = 0 (connection reported absent or unknown), black entries denote c_{ij} = 1 (connection present), and gray entries mark the main diagonal with entries c_{ii} = 0. Row entries of the matrix are sources ("efferents") and column entries are targets ("afferents"). **(A)** Macaque visual cortex, after Felleman and van Essen (1991). **(B)** Macaque cortex, after Young (1993). **(C)** Cat cortex, after Scannell et al. (1999).

were deleted from the matrix, resulting in N = 71 and K = 746. Note that most of the areas and connections of the macaque visual cortex form a subset of this matrix.

Cat Cortex

The connection matrix (Fig. 1C) was transcribed from the original article by Scannell et al. (1999). We deleted area "Hipp" (hippocampus) and all cortico-thalamic pathways. For the large-scale analysis, density information was discarded and all pathways were encoded as either present or absent. The resulting matrix has N = 52 and K = 820.

Cat Cortex: Density-Based Connectivity Data Sets

The matrix of connections for cat cortex (Scannell et al., 1999) contained information on the density or strength of pathways, encoded in an ordinal scheme with ratings of 3, 2, 1, and 0 (indicating decreasing connection density). Using this information we generated a connection matrix in which each area was replaced by 10 elements (vertices), arranged along the main diagonal using the original ordering scheme, resulting in N = 520. For each original pathway with strength c_{ij}, the corresponding 10×10 patch of connections was assigned the same strength c_{ij}. The resulting ordinal matrix CIJ_{ord} (Fig. 2A) was then converted to a scaled connection matrix CIJ_{scl} by substituting ordinal connection strengths with scaled values representing a connection probability according to

$$CIJ_{scl} = \psi_1(CIJ_{ord}=1) + \psi_2(CIJ_{ord}=2) + \psi_3(CIJ_{ord}=3)$$

with ψ_1, ψ_2 and ψ_3 denoting the scaling factors (observing $0 < \psi_1 < \psi_2 < \psi_3 \leq 1$). The scaled matrix CIJ_{scl} is then converted to a binary connection matrix CIJ_{bin} (Fig. 2B).

Probabilistic Connectivity Data Sets

Connection matrices of intra-areal cortico-cortical connections are created using a probabilistic generating function. We consider a square array of elements (vertices), imposing toroidal boundary conditions to exclude edge effects. Each element maintains connections to other elements in the array according to a rotationally symmetric (isotropic) Gaussian probability profile, with a standard deviation of σ_g. The connection matrix of the array is generated by random assignment of binary connections according to this Gaussian profile. Each element maintains, on average, an equal number of connections.

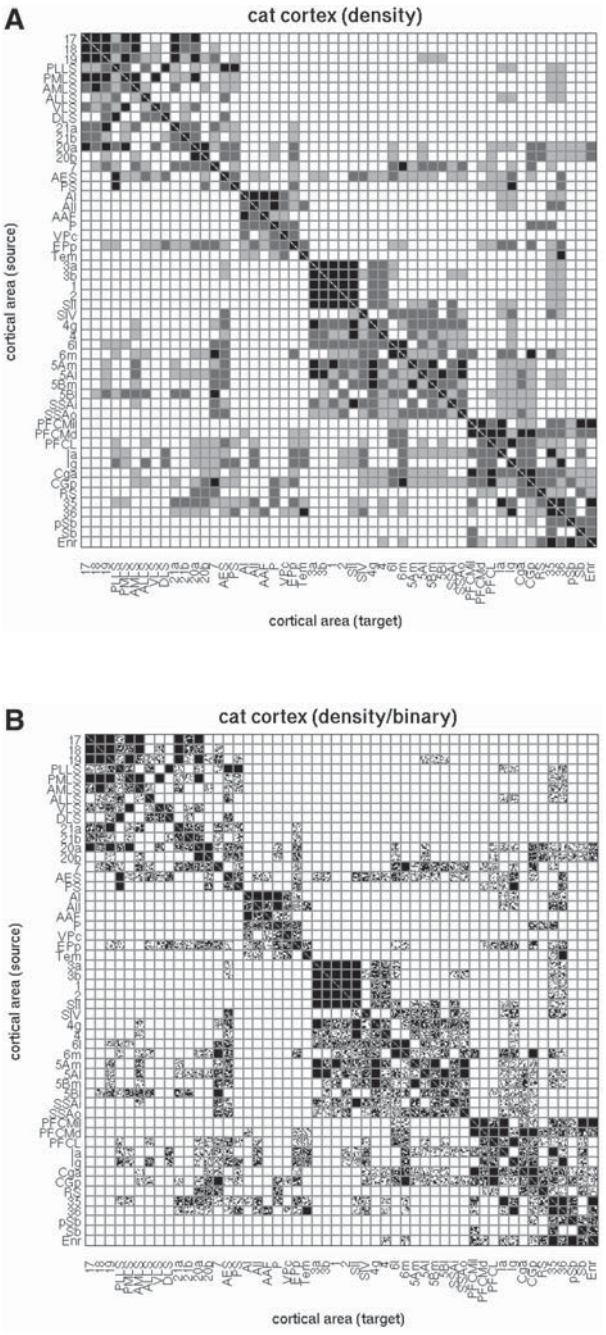

Fig. 2. Density-based connectivity data set for cat cortex. **(A)** Cat cortex, including density information as recorded in Scannell et al. (1999), with minor modifications as described in the text. The image represents the ordinal density matrix CIJ_{ord} (white = 0, light gray = 1, dark gray = 2, black = 3). **(B)** Binary density matrix CIJ_{bin}, with $\psi_1 = 0.33$, $\psi_2 = 0.67$, $\psi_3 = 1.00$.

Reference Cases: Random and Lattice Matrices

Random connection matrices are generated by assigning connections with uniform probability $K/(N^2-N)$, while omitting self-connections. Lattice matrices are generated by filling all entries of the connection matrices directly adjacent to the main diagonal until the limit of K connections is reached. For example, if K = 2N, this procedure would result in nearest-neighbor connectivity (ring topology). Special kinds of random and lattice matrices that preserve the in-degree and out-degree for each vertex are generated from the original anatomical connection matrices by a Markov-chain algorithm (Maslov and Sneppen, 2002; Milo et al., 2002). For random matrices, a pair of vertices (i_1,j_1) and (i_2,j_2) is selected for which $c_{i_1 j_1} = 1$, $c_{i_2 j_2} = 1$, $c_{i_1 j_2} = 0$, and $c_{i_2 j_1} = 0$. Then we set $c_{i_1 j_1} = 0$, $c_{i_2 j_2} = 0$, $c_{i_1 j_2} = 1$, and $c_{i_2 j_1} = 1$. This is repeated until the connection topology of the original matrix is randomized. For lattice matrices, the same Markov procedure is employed, however swaps are only carried out if the resulting matrix has non-zero entries that are located closer to the main diagonal (approximating a lattice topology). This is implemented as a probabilistic optimization using a weighted cost function for distance.

Graph Theory Methods

We utilize a set of graph theoretical methods described in Sporns (2002) and based on classical digraph theory (Harary, 1968; Chartrand and Lesniak, 1996) as well as methods specifically developed for the analysis of small-world networks (Watts and Strogatz, 1998; Watts, 1999).

Path Length

Paths are ordered sequences of distinct edges and vertices, linking a source vertex *j* to a target vertex *i* (Fig. 3A,B). The length of a path is defined as the number of distinct directed edges. The characteristic path length λ of a graph is

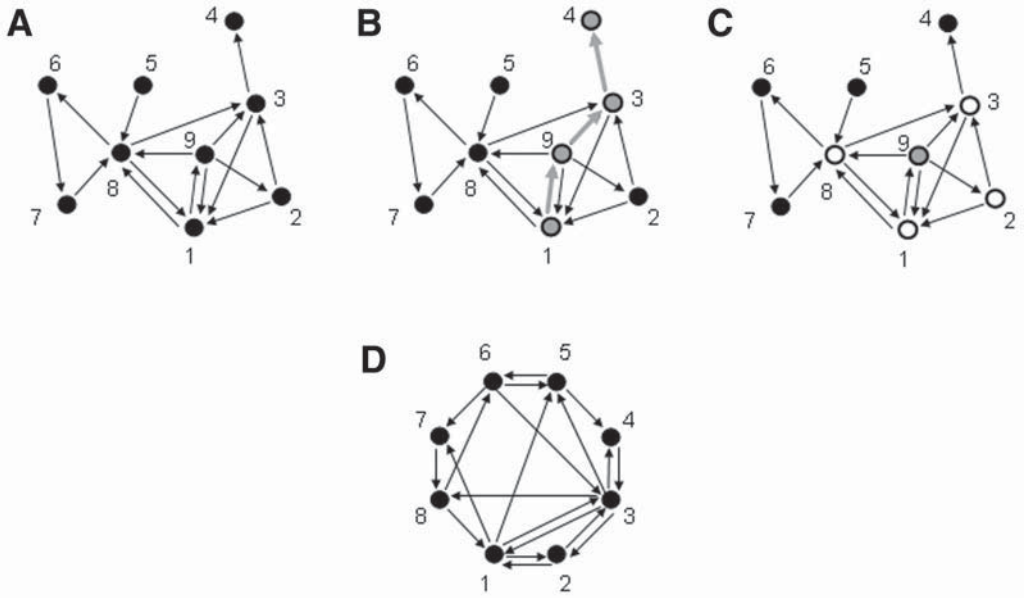

Fig. 3. Illustration of key graph-theoretical measures used in the paper. **(A)** Digraph composed of N = 9 vertices and K = 16 directed edges. **(B)** Path from vertex 1 to vertex 4 of length 3, denoted {1,9,3,4}, containing the directed edges (1,9), (9,3), and (3,4). The length of this path corresponds to the distance from vertex 1 to 4. An alternative path from 1 to 4 is {1,8,3,4} and another path of length 4 is {1,9,8,3,4}. **(C)** Cluster index of vertex 9. This vertex's neighbors are 1, 2, 3, and 8, which maintain 6 connections among them out of 12 possible (4^2–4). This results in a cluster index of 6/12 = 0.5. **(D)** Digraph composed of N = 8 vertices and K = 20 directed edges. The graph contains 8 distinct cycles of length 3 {1,7,8,1}, {1,2 3,1}, {3,2,1,3}, {3,5,4,3}, {6,7,8,6}, {3,8,6,3}, {3,5,6,3}, and {1,3,8,1}, obtained by counting structural motifs (see text for details). Note that following the method published by Milo et al. (2002), reveals only three cycles: {1,7,8,1}, {3,8,6,3}, and {6,7,8,6}. The cycle probabilities for this graph are $p_{cyc}(2) = 0.5$ and $p_{cyc}(3) = 0.5217$. Counting all paths yields a total of 56 paths of length 2, of which 46 are non-cyclic, and a total of 24 cycles of length 3 resulting in $p_{cyc}(3) = 24/46$. Note that to obtain valid cycle probabilities one must count each cycle of length q q times.

the average length of the shortest possible paths linking any pair of its vertices. The length of the shortest path from vertex *j* to *i* is also called the distance d_{ij}. All distances d_{ij} compose the distance matrix D of the graph. Thus, λ is equal to the average of all entries d_{ij} of the distance matrix D. The path length of a vertex $\lambda(v)$ is defined as the average distance between this vertex and all other vertices of the graph (excluding d_{ii}).

Cluster Index

The cluster index (originally called "clustering coefficient" by Watts and Strogatz, 1998) of a vertex v indicates how many connections are maintained between this vertex's b_v neighbors (Fig. 3C). The vertex's cluster index $\gamma(v)$ is defined as the ratio of actually existing connections among the b_v neighbors and the maximal number of such connections possible (b_v^2–b_v). Note that $0 \leq \gamma_v(v) \leq 1$. The average of the cluster indices for each vertex is the cluster index γ of the graph.

Scaling of λ and γ

Random and lattice networks represent topologies that lie at the extreme ends of a continuous spectrum ranging from totally disordered (random) to totally regular (lattice). The comparison of values for λ and γ of a given neuroanatomical network to these extreme

topologies provides information about the extent to which the network incorporates random or regular structural features. It is generally the case (Watts, 1999) that, for equivalent (and sufficiently large) N and K, $\lambda_{random} << \lambda_{lattice}$ and $\gamma_{random} << \gamma_{lattice}$. Scaled values for λ and γ for a given network of unknown topology are calculated as:

$$\lambda_{scl} = (\lambda_{network} - \lambda_{random})/(\lambda_{lattice} - \lambda_{random})$$

$$\gamma_{scl} = (\gamma_{network} - \gamma_{random})/(\gamma_{lattice} - \gamma_{random})$$

Generally, for networks with topologies that are intermediate between random and lattice structures, λ_{scl} and γ_{scl} will be between 0 and 1.

Cycles

Cycles are paths that begin and end in the same vertex. The abundance of cycles of different lengths in a given network is quantified using two different methods (Fig. 3D). The first method determines the probability $p_{cyc}(q)$ that a non-cyclic path of length q–1 can be continued as a cycle of length q by the addition of one edge (Sporns et al., 2000; Sporns, 2002). Note that $0 \leq p_{cyc}(q) \leq 1$. The second method counts the number of occurrences of a cycle of given length (called a "motif") within the network, discounting duplications owing to symmetries. Counting of motifs within graphs was recently introduced by Milo et al. (2002). We note that their method gives different results from the one used in the present article: Their algorithm counts only identical matches between motifs and sub-graphs, while occurrences of motifs that are part of larger structures are not counted. Figure 3D illustrates results for counting cycles obtained by these various methods in a simple example network with N = 8 and K = 20.

Web Resources

Neuroanatomical data sets and a Matlab toolbox containing most of the functions used in this paper can be found at www.indiana.edu/~cortex/lab.htm.

Results

Large-Scale Connectivity Data Sets

All large-scale connectivity data sets examined in this study are shown in Fig. 1 and Fig. 2 (for area abbreviations see the corresponding original publications). Table 1 summarizes the results of a comprehensive structural analysis of these matrices using graph theory methods. In all cases, the original anatomical connection matrices were compared against random and lattice matrices of equal N and K. This allows the scaling of path length λ and cluster index γ by using random and lattice matrices as reference cases ("benchmarks"). Our approach is consistent with Watts and Strogatz' (1998) original criterion of $\gamma_{network} >> \gamma_{random}$ and $\lambda_{network} \approx \lambda_{random}$. For all three large-scale connection matrices, we found that values for λ_{scl} are closer to those for random networks, and values for γ_{scl} are closer to those of lattice networks. This indicates that large-scale connection matrices are characterized by very short average distances between any two vertices while at the same time maintaining a high degree of clustering. A comparison to random and lattice matrices with distributions of in-degrees and out-degrees that are identical to those of the corresponding neuroanatomical matrices (i.e., preserving the distributions of inputs and outputs to each element while altering their global pattern) yields fundamentally the same result (*see* Table 1). Thus, low λ and high γ for large-scale matrices cannot be explained by their degree distributions (local vertex statistics), but depend on the global arrangement of the connection pattern.

Values for λ and γ in Table 1 represent averages over all brain areas represented in the networks. Individual brain areas, however, show significant variations for these measures. Figure 4 displays values for $\lambda(v)$ and $\gamma(v)$ for individual brain areas in macaque visual cortex (Fig. 4A), macaque cortex (Fig. 4B), and cat cortex (Fig. 4C). In all three large-scale matrices,

Table 1. Path Length (λ, λ_{scl}) and Cluster Index (γ, γ_{scl}) for Large-Scale Connection Matrices of Cortico-Cortical Pathways

Topology	λ	γ	λ_{scl}	γ_{scl}
MVC	1.7256	0.5313	0.2188	0.5645
$R_{30,311}$	1.6680 (0.0038)*	0.3616 (0.0048) *		
$L_{30,311}$	1.9313 (0.0018)*	0.6622 (0.0000) *		
$Rio_{30,311}$	1.6880 (0.0033)*	0.4305 (0.0059) *		
$Lio_{30,311}$	1.8190 (0.0391)	0.6214 (0.0243)		
MC	2.3769	0.4614	0.1927	0.6117
$R_{71,746}$	2.0310 (0.0051)*	0.1497 (0.0030) *		
$L_{71,746}$	3.8262 (0.0099)*	0.6593 (0.0002) *		
$Rio_{71,746}$	2.1159 (0.0133)*	0.2409 (0.0047) *		
$Lio_{71,746}$	2.8901 (0.1173)*	0.8992 (0.0211) *		
CC	1.8114	0.5514	0.2498	0.6292
$R_{52,820}$	1.7014 (0.0013)*	0.3103 (0.0026) *		
$L_{52,820}$	2.1418 (0.0024)*	0.6933 (0.0000) *		
$Rio_{52,820}$	1.7217 (0.0037)*	0.4023 (0.0030) *		
$Lio_{52,820}$	1.8570 (0.0283)	0.5893 (0.0172)		

Measures for reference cases represent means and standard deviations (in brackets) for 10 exemplars. Topologies: MVC = macaque visual cortex (Fig. 1A), MC = macaque cortex (Fig. 1B), CC = cat cortex (Fig. 1C), $R_{N,K}$ = random, $L_{N,K}$ = lattice, $Rio_{N,K}$, $Lio_{N,K}$ = random, lattice matrices with in-degree and out-degree distribution preserved. Statistical significance for all comparisons between cortical matrices and random, lattice, Rio, or Lio matrices marked by "*" are $p<0.001$, the remaining comparisons are $p<0.05$.

there is a strong tendency for a positive correlation between $\lambda(v)$ and $\gamma(v)$. For example, in macaque visual cortex, area V4 exhibits markedly low path length and low cluster index, while other areas (e.g. V1, V4t, STPa) have both high $\lambda(v)$ and $\gamma(v)$. Interestingly, with the exception of area STPa, all areas generally considered to be members of the ventral stream of primate visual cortex (VOT, CITd, CITv, PITd, PITv, AITd, AITv, TH, STPp, and TF—with V4 often included; *see* Felleman and van Essen, 1991 and discussion in Hilgetag et al., 2000) are found below the regression line (Fig. 4A), indicating that these areas are as reachable but are less clustered than their dorsal stream counterparts. The positive correlation between λ and γ may be explained in part by a strong tendency, found in all three large-scale connection matrices, for brain areas with a large number of neighbors to have relatively low γ (Fig. 4) and λ (not shown). Area V4 in macaque visual cortex, for example, maintains 21 incoming and outgoing connections, but has a $\gamma_v(V4) = 0.3190$. The connectivity pattern of V4 is highly diverse, including areas in dorsal and ventral streams of the visual cortex and constituting a broad set of neighbors that do not form a single "clique." Similar relationships are seen in other large-scale matrices. In the entire connection system of macaque cortex, areas with markedly low λ and γ include A7b, LIP, TPT, FEF, and A46, all of which mediate interactions between various sensory and motor systems (Young, 1993). In the cat cortex, areas with low λ and γ include multimodal areas 7, AES, and EPP, as well as fronto-limbic areas Ia, Ig, 35, 36, and CGp

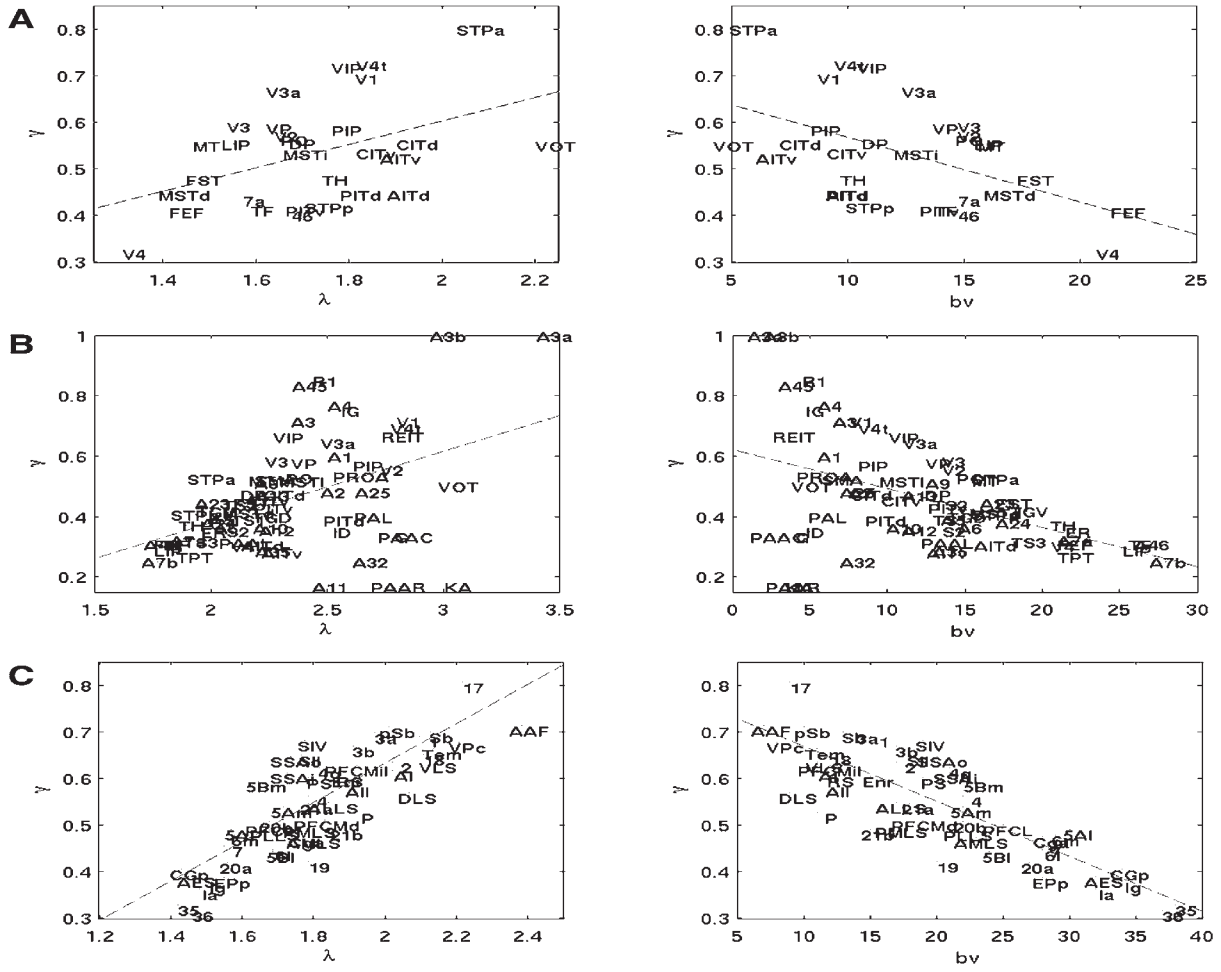

Fig. 4. Correlations between the path length λ, the cluster index γ and the number of neighbors per vertex b_v, for individual brain regions of the macaque visual cortex **(A)**, macaque cortex **(B)**, and cat cortex **(C)**.

(classified according to Scannell and Young, 1993). Again, these areas maintain a relatively large number of projections with several different sensory and motor systems, resulting in an abundance of short paths and relatively reduced clustering. The observed correlations between λ, γ and the size of the neighborhood are absent in random networks. Lattice networks do not show much variation in λ and γ across vertices, owing to their mode of construction.

Table 2 summarizes the relative abundance of short cycles of length q = 2, 3, and 4, obtained by enumerating their occurrence in each network, or by calculating the cycle probability $p_{cyc}(q)$ from path distributions. Both methods revealed that large-scale connection matrices have an overabundance of short cycles relative to their incidence in random matrices with equal N and K. In some cases, the abundance of short cycles in neuroanatomical matrices even exceeded the corresponding measures in lattice matrices.

Table 2. Number of Cycles in Large-Scale ConnectionMatrices of Cortico-Cortical Pathways

Topology	2	3	4	$p_{cyc}(2)$	$p_{cyc}(3)$	$p_{cyc}(4)$
MVC	121	550	3726	0.7781	0.4945	0.4407
$R_{30,311}$	57 (5)	376 (9)	2673 (99)	0.3633 (0.0315)	0.3624 (0.0073)	0.3559 (0.0079)
$L_{30,311}$	150	655	3440	0.9646 (0.0000)	0.6722 (0.0025)	0.5393 (0.0047)
MC	308	1231	9226	0.8257	0.3903	0.3150
$R_{71,746}$	56 (6)	384 (17)	2908 (95)	0.1493 (0.0169)	0.1498 (0.0055)	0.1491 (0.0024)
$L_{71,746}$	255	1600	8540	0.9517 (0.0000)	0.6735 (0.0024)	0.5394 (0.0047)
CC	301	2302	25333	0.7341	0.4841	0.4258
$R_{52,820}$	130 (7)	1299 (23)	14748 (339)	0.3176 (0.0164)	0.3075 (0.0046)	0.3077 (0.0039)
$L_{52,820}$	404	2828	25032	0.9854 (0.0000)	0.6998 (0.0009)	0.5864 (0.0017)

The number of distinct occurrences of cycles of length q=2, 3, and 4 was determined by counting of motifs (see text for details) and the cycle probability for cycles of length q=2, 3, and 4 was calculated by enumerating all distinct paths of length q and q−1. Measures for reference cases represent means and standard deviations (in brackets) for 10 exemplars. Statistical significance is $p<0.001$ for all comparisons between cortical matrices and random or lattice matrices. Topologies: MVC = macaque visual cortex (Fig. 1A), MC = macaque cortex (Fig. 1B), CC = cat cortex (Fig. 1C), $R_{N,K}$ = random, $L_{N,K}$ = lattice.

We examined the distributions of in-degrees and out-degrees for evidence of a scale-free architecture, which is characterized by a power law distribution ("fat tail") of the number of vertices with a given number of incoming and/or outgoing edges. Only the matrix of interareal pathways of the macaque cortex revealed hints of a possible scale-free distribution, primarily through the existence of several "hubs", i.e., areas with very high numbers of incoming and outgoing connections, including areas A7b, A46, and LIP with degrees of 53, 50, and 47, respectively (and correspondingly large and diverse neighborhoods). Other large-scale matrices do not exhibit clear candidates for hubs, perhaps because of the relatively small size N. Notably, all large-scale matrices have degree distributions with significantly higher variance than corresponding random (or lattice) networks.

Figure 2 shows an example of a large-scale cortical connection matrix in which (a) the individual brain areas were replaced by sets of elements and (b) the individual pathways were replaced by sets of connections with a local density corresponding to the recorded density of the pathway. Such information is currently only available for the matrix of connections within cat cortex (Scannell et al., 1999; *see also* BAMS, 2003). Since the assignment of connection densities in the original publications is ordinal, we used different combinations of scaling factors ψ_1, ψ_2 and ψ_3 (observing $0 < \psi_1 < \psi_2 < \psi_3 \leq 1$) to examine structural properties of the resulting graphs. Table 3 summarizes graph theory measures obtained for these density-based matrices. Despite large variations in the numerical values of ψ_1, ψ_2 and ψ_3 the corresponding connection matrices show robust small-world properties with short path lengths λ_{scl} and a high degree of clustering γ_{scl}. The small world effect is rather more compelling. For settings of $\psi_1 = 0.05$, $\psi_2 = 0.25$ and $\psi_3 = 0.5$, two randomly selected vertices are on average separated by only 2.3 steps, despite N = 520 and a connection density of approx 6%.

Table 3. Path length (λ, λ_{scl}) and Cluster Index (γ, γ_{scl}) for Probabilistic Large-Scale Connection Matrices of Cat Cortex

Topology	λ	γ	λ_{scl}	γ_{scl}
$CCdens_{0.33,0.67,1.00}$	1.9477 (0.0008)	0.4132 (0.0013)	0.1037	0.4105
$R_{520,49917}$	1.8154 (0.0005)	0.1849 (0.0006)		
$L_{520,49917}$	3.2231 (0.0076)	0.7410 (0.0007)		
$CCdens_{0.05,0.25,0.50}$	2.3817 (0.0061)	0.2087 (0.0016)	0.0572	0.2171
$R_{520,17711}$	2.0343 (0.0032)	0.0656 (0.0006)		
$L_{520,17711}$	8.1125 (0.0591)	0.7248 (0.0019)		

Two sets of values correspond to matrices generated with scaling factors $\psi_1 = 0.33$, $\psi_2 = 0.67$ and $\psi_3 = 1.00$ (top, *see* Fig. 2B) and $\psi_1 = 0.05$, $\psi_2 = 0.25$ and $\psi_3 = 0.5$ (bottom), respectively. The resulting matrices haves sizes of N = 520, K = 49917 (138) and N = 520, K = 17711 (131), respectively. The corresponding average connection densities are 0.1850 and 0.0656. All values, including those of random and lattice matrices, are averages of 10 exemplars and correspond to mean and standard deviation (in brackets). Statistical significance is $p<0.001$for all comparisons between cortical matrices and random or lattice matrices. Topologies: $CCdens\psi_{1,2,3}$ = cat cortex density matrix (Fig. 2), $R_{N,K}$ = random, $L_{N,K}$ = lattice.

Probabilistic Connectivity Data Sets

Cortico-cortical connections at the level of small populations or single neurons have distinct and non-uniform spatial distributions. In many of the cases examined either anatomically or physiologically, the metric distance between neurons is a key determinant of the probability of mono-synaptic connection (*see* "Discussion"). We generated sets of connection matrices that implemented different probabilistic connection schemes and examined them using graph theory methods. Three main topologies were compared. In the first case ("all local") all connections were assigned according to Gaussian probability profiles (*see* Fig. 5). In the second case ("local plus uniform"), a proportion of connections were generated between uniformly distributed and randomly chosen units irrespective of their metric distance (*see* Fig. 6). In the third case ("local plus long-range"), two maps containing "all local" Gaussian-distributed connections were reciprocally linked by "long-range" connections distributed according to a second Gaussian profile (*see* Fig. 7). This created networks resembling two topographic cortical maps with intra-areal and inter-areal connections forming a simple topological hierarchy.

Gaussian connection profiles in "all local" networks did not generate small-world connectivity patterns. Figure 5 shows results obtained by systematically varying the width σ_g of the Gaussian profile and generating a spectrum of networks consisting of a single square array of 40×40 units. One grid unit of the network is taken to represent a small cortical cell population occupying a region with a diameter of approx 25 μm, leading to overall dimensions of about 1×1 mm. The extreme cases are networks in which all connections link neighboring units (σ_g =1.25) and networks in which connections are spread out across the array ($\sigma_g = 39$). These cases closely correspond to lattice and random connection topologies, respectively, and their path lengths and cluster indices were used for scaling of intermediate cases. Values of λ_{scl} and γ_{scl} were high for $\sigma_g = 1.25$ and low for $\sigma_g = 39$, but did not reveal small-world architectures (low λ_{scl} and high γ_{scl}) for any of the intermediate networks (Fig. 5).

A small admixture of "uniform" connections linking pairs of units irrespective of their metric

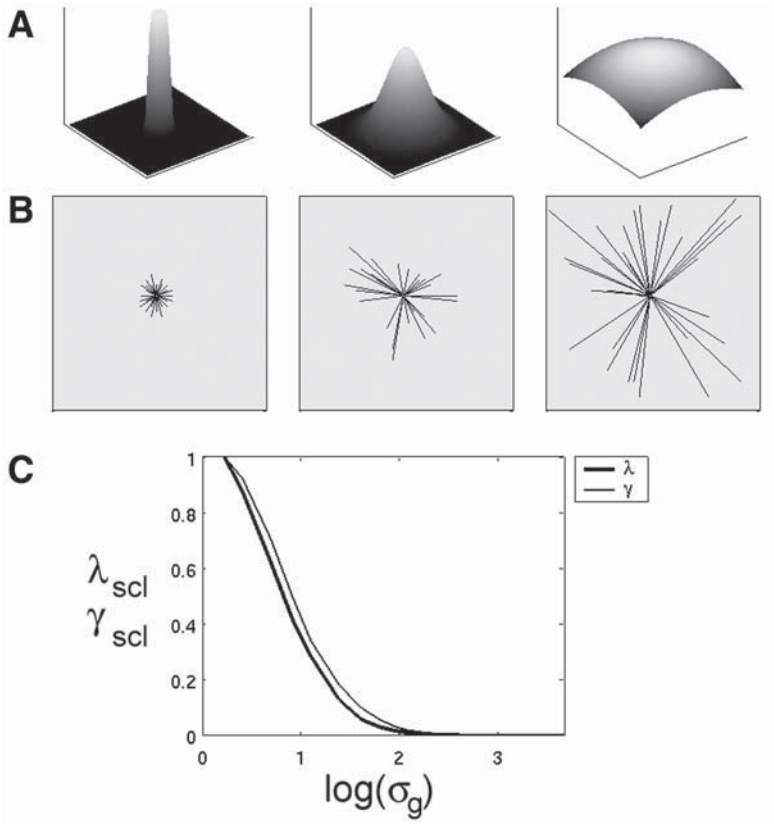

Fig. 5. Probabilistic connectivity data sets—"all local" connections within a single cortical area. **(A)** Gaussian probability profiles used to assign connections, with σ_g = 1.25, σ_g = 6 and σ_g = 39 (left to right). **(B)** Plot of spatial distribution of efferent connections (approx 32) for a single representative neuron. **(C)** Scaled path length λ_{scl} (thick line) and cluster index γ_{scl} (thin line) for networks generated with Gaussian probability profiles of different standard deviation σ_g.

distance in the array drastically lowered the path length while leaving the cluster index largely unaffected. Figure 6 displays structural properties of a series of networks with varying amounts of uniformly distributed long-range connections added to local Gaussian connections. Small proportions of long-range connections on the order of 10% or less resulted in networks with relatively low λ_{scl} and high γ_{scl}.

While some intra-cortical connections may range over distances of several millimeters (Hellwig, 2000), it is unlikely that significant numbers of intra-cortical connections are generated with spatially uniform probability. A more realistic pattern consists of a combination of local intra-areal and global inter-areal connections (Fig. 7). Analysis of such patterns revealed the emergence of small-world attributes. In the example displayed in Fig. 7, we created connection patterns linking elements in two areas, with dimensions of 40×40 elements each and toroidal boundary conditions. With an average of 32 intra-areal and 8 inter-areal connections per unit the two area network had N = 3200, K = 127,834, and a connection density of 0.0125. Intra-areal connections were distributed according to a Gaussian distribution with σ_g = 2 and inter-areal connections had σ_g = 8. Graph theoretical analysis of the network's connection matrix revealed that the graph was fully

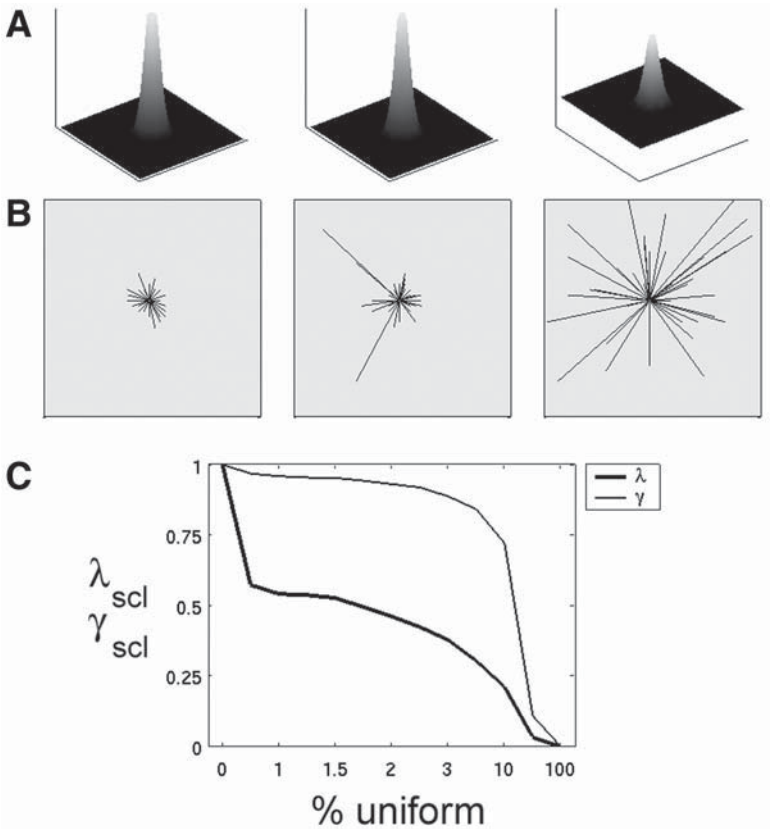

Fig. 6. Probabilistic connectivity data sets—"local plus uniform" connections within a single cortical area. **(A)** Probability profiles used to assign connections, composed of a Gaussian and a uniform component. The Gaussian component has σ_g = 2 throughout. The uniform component comprises 0, 10 and 100 percent of the total number of connections (left to right). **(B)** Plot of spatial distribution of efferent connections (approx 32) for a single representative neuron. **(C)** Scaled path length λ_{scl} (thick line) and cluster index γ_{scl} (thin line) for networks generated with Gaussian probability profiles and different proportions of uniformly distributed connections.

connected and had $\lambda = 2.8755$ and $\gamma = 0.1919$. Creating equivalent random and lattice topologies allowed scaling of λ and γ, with $\lambda_{scl} = 0.185$ and $\gamma_{scl} = 0.543$, revealing a small world network. Low values for λ_{scl} and high values for γ_{scl} are found for many combinations of intra- and inter-areal connection density and spread.

Discussion

Small Worlds and Cortical Function

As in many other biological systems, structure and function of the cerebral cortex are intimately related. Cortical neuroanatomy, the patterning of neural connections linking individual cells, cell populations, and brain areas, is a key determinant of the capacity of cortex to generate and integrate information. In this article we used a variety of tools to analyze the structure of a broad spectrum of cortical connectivity patterns, ranging from large-scale systems of inter-regional pathways to probabilistic connection matrices for combinations of inter-areal and intra-areal connections. Our analysis included the comparison of actual cortical connection matrices to reference cases that are generated under different sets of statistical assumptions. This approach allowed the

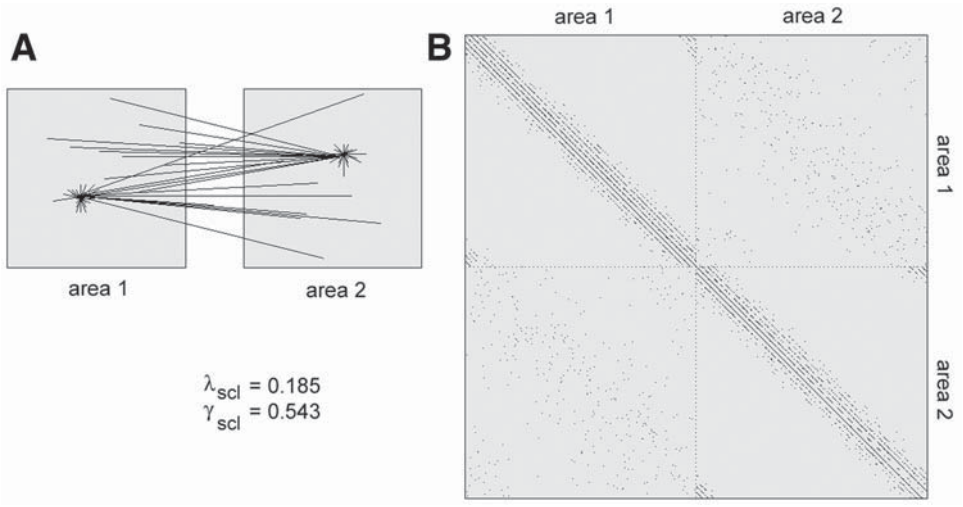

Fig. 7. Probabilistic connectivity data sets—"local plus long-range" connections linking neurons within and between two cortical areas. **(A)** Plot of spatial distribution of efferent connections (approx 32 intra-areal and 8 inter-areal) for two representative neurons located in each of the two areas. Connections were assigned using Gaussian probability profiles with σ_g = 2 (intra-areal) and σ_g = 8 (inter-areal). **(B)** Connection matrix for the entire network (N = 3200, K = 127834). Note the concentration of connections near the main diagonal (local spread) and the self-similar pattern in the four quadrants.

identification and comparison of structural features that distinguish neurobiological patterns from random or lattice (e.g., nearest-neighbor) topologies. This comparison is essential as absolute values for path lengths and cluster indices often are not, by themselves, indicative of the presence of small-world connectivity patterns.

We detect robust small world properties in every cortical network examined in this study. The present analysis confirms and extends the earlier studies and published data by Sporns et al. (2000) and Hilgetag et al. (2000). The small world topology is characterized by two main coexisting features. First, the neighborhood surrounding most neuronal elements shares many more interconnections than would be expected by chance (high γ_{scl}). Second, pairs of neuronal elements are linked by short paths, despite large network size and sparse connectivity (low λ_{scl}). The pervasiveness of small world attributes in cortical networks points to their central functional role. High clustering promotes functional overlap of densely connected neuronal elements, which are functionally segregated from one another and constitute building blocks (topological modules) of the cortical architecture. Short paths promote effective interactions between neuronal elements within and across cortical regions, which are essential for functional integration. Thus, the coexistence of high clustering and short path length in cortical networks assures the effective integration of multiple segregated sources of information. In computer simulations (Sporns et al., 2000), small world topologies emerge when networks are optimized for complexity, a measure of how well a network combines functional segregation and integration (Tononi et al., 1998; Sporns and Tononi, 2002).

A striking aspect of cortical connectivity is that it contains structure across different spatial scales, ranging from large-scale interregional pathways to local circuits. Densely

and locally connected topological "modules" combine at several spatial scales to form larger units of varying degree of cohesiveness. Our analysis provides preliminary indications that the network topology of cortex incorporates aspects of heterogeneity ("randomness") and homogeneity ("regularity") at several spatial scales, including large-scale cortical systems and local intra-areal networks. Nested and embedded modules of densely coupled and thus functionally interrelated elements are combined and recombined across multiple levels. Modular and hierarchical organization appears to be a robust feature of other biological systems such as metabolic and protein networks (Ravasz et al., 2002; Rives and Galitski, 2003).

Plotting individual variations in path length $\lambda(v)$ and cluster index $\gamma(v)$ for each brain area (Fig. 4) may provide a new way to classify cortical areas as either highly specialized (involved primarily in local processing within a given modality) or integrative (involved in multimodal association, or cross-model communication). We observed a fairly strong correlation between $\lambda(v)$ and $\gamma(v)$ for all large-scale cortical connection matrices. Areas with low $\lambda(v)$ and low $\gamma(v)$ tended to maintain larger numbers of pathways with a greater diversity of other brain areas. For example, parietal area A7b in macaque cortex has $\lambda(A7b) = 1.7714$ and $\gamma(A7b) = 0.2500$ and connects to 28 other areas including somato-sensory area A5, frontal eye fields FEF, temporal visual areas TF and TH, and motor and premotor cortex areas A4 and A6 (*see also* Lewis and Van Essen, 2000). Its functional neuronal properties are highly complex and multimodal (Graziano et al., 1999), in accordance with its widespread connection profile. On the other hand, areas with high $\lambda(v)$ and high $\gamma(v)$ tended to maintain smaller numbers of pathways, mostly to brain areas that are strongly functionally related. For example, area A3a of the somato-sensory cortex has $\lambda(A3a) = 3.4714$ and $\gamma(A3a) = 1.0000$ and connects to only two other areas (somato-sensory areas A1 and A2). This distinction of more specialized and more integrative cortical areas according to the statistics of their connectional relationship with the rest of the network is consistent with the notion that the anatomical "fingerprint" of an area defines its functionality (Passingham et al., 2002). The approach of defining characteristics of brain areas by assigning connectivity measures was pioneered and applied in a different context by Kötter and Stephan (2003).

Design of Probabilistic Connection Patterns

We adopted Gaussian probability profiles for assigning both intra- and inter-areal connections in probabilistic connection patterns. Detailed anatomical studies demonstrate an exponential or Gaussian fall-off of connection probability with increasing spatial separation of two neurons (Braitenberg and Schüz, 1998; Hellwig, 2000; Liley and Wright, 1994). Such a probabilistic model does not incorporate actual developmental or growth processes guiding formation of synapses, or experience-dependent refinement of cortical connections. Small world topologies were found in networks that contained mixtures of local (Gaussian) and some form of long-range connections. These long-range connections could be added either as spatially uniformly distributed links or through introducing reciprocal coupling (again with a Gaussian spatial profile) between two areas. The latter type of connectivity is ubiquitous within the cortex.

Small world connectivity may favor the emergence of complex neural dynamical states within and between cortical areas. In a previous simulation study, we showed that small world connection topologies were capable of generating neuronal dynamics with high complexity, i.e., simultaneous presence of local (segregated) and global (integrated) structure (Sporns, 2004). The rich taxonomy of nonlinear phenomena encountered in networks of coupled nonlinear

neuronal units (e.g., Breakspear et al., 2003) needs to be investigated further, for example by simulating small world networks with realistic nonlinear neuronal dynamics.

Distance Between Neurons

Distance between neurons is an important but rather subtle concept. In physically implemented networks, we must distinguish between metric and topological distance. The former expresses the physical separation (in μm or mm) between neurons, while the latter captures the "directness" of causal interaction through synaptic linkages. In the cortex, metric and topological distances are clearly related, but in terms of functional and informational considerations, it is topological distance that most directly determines the strength of functional interactions. Absence of any path between two neurons precludes causal effects of one on the other, even if their metric distance is small (discounting potential chemical communication through intercellular space or the vasculature). If a path is present, its functional impact depends strongly on its length, with longer paths increasingly unlikely to impart any causal influence on target neurons. The effectiveness of a path is also a function of the strengths of the synaptic links, as well as the excitability and responsiveness of its constituent neurons, all factors that are outside the scope of classical graph theory.

Scale-Free or Single-Scale?

We found little or no evidence of scale-free degree distributions in either large-scale or cortico-cortical probabilistic connection matrices (however, *see* Martin et al., 2001 for a different view). While several "hubs" appeared to exist within the macaque cortex, such highly connected brain regions were less evident within macaque visual cortex or cat cortex. There is currently very little empirical information on the number of connections per unit at the level of small cortical populations or single cells. In our probabilistic approximations of cortico-cortical connections, each unit made connections according to the same probability profile resulting in approximately equal numbers of incoming and outgoing connections. This is in accordance with a relatively constant number of synapses per cortical pyramidal cell (on the order of 10,000) and inconsistent with a scale-free architecture at the level of anatomical connections. Scale-free architectures emerge naturally as a result of preferential attachment during network growth (Albert and Barabasi, 2002). However, physical constraints on the number of afferent connections a neuron can support render preferential attachment *alone* an unlikely mechanism in neural development. Limited capacity of vertices to add links has been shown to result in a disappearance of the power law regime (Amaral et al., 2000). However, it is still possible that scale-free or "broad-scale" (Amaral et al., 2000) architectures will be found once large-scale connectional information is refined to include missing connections and areas.

Conclusion

Numerous studies in natural, social and technological systems have shown that small world networks give rise to interesting functional and dynamic properties, including generating complex dynamics (Sporns, 2004), an increased propensity for synchronization (Barahona and Pecora, 2002), efficient information exchange (Latora and Marchiori, 2001), and efficient navigability of information and social networks (Kleinberg, 2000). We hypothesize that the small world topology plays a central role in cortical information processing as well. This role will become more evident as we begin to relate structural analyses of networks to the dynamical patterns and states they generate and sustain. Neuroimaging and electrophysiological techniques are revealing in ever more detail the complex and fleeting

patterns of interactions between specialized regions of cortex that unfold during the functioning of the brain. Information integration within the brain, and the cohesiveness of mental awareness itself, ultimately depends on the structure of the underlying network, the small world of the cerebral cortex.

Acknowledgments

O.S. was supported by US government contract NMA201-01-C-0034, J.Z. was supported by the Indiana University SROP program and a McNair fellowship. The views, opinions, and findings contained in this paper are those of the authors and should not be construed as official positions, policies, or decisions of NIMA or the US government.

References

Albert, R., Jeong, H., and Barabasi, A. -L. (1999) Diameter of the world wide web. Nature 401, 130–131.

Albert, R. and Barabasi, A. -L. (2002) Statistical mechanics of complex networks. Rev. Mod. Phys. 74, 47–97.

Amaral, L. A. N., Scala, A., Barthelemy, M., and Stanley, H. E. (2000) Classes of small-world networks. Proc. Natl. Acad. Sci. USA 97, 11149–11152.

Ascoli, G. A. (2002) *Computational Neuroanatomy. Principles and Methods*. Humana Press, Totowa, NJ.

BAMS (2003) Brain Area Management System. http://brancusi.usc.edu/bkms/.

Barabasi, A. -L. (2002) Linked. The New Science of Networks. Perseus, Cambridge, MA.

Barahona, M., and Pecora, L. M. (2002) Synchronization in small-world systems. Phys. Rev. Lett. 89, #054101.

Bressler, S. L. (1995) Large-scale cortical networks and cognition. Brain Research Reviews 20, 288–304.

Bota, M., Dong, H. -W., and Swanson, L. W. (2003) From gene networks to brain networks. Nature Neuroscience 6, 795–799.

Braitenberg, V. and Schüz, A. (1998) Cortex: Statistics and Geometry of Neuronal Connectivity. Springer, Berlin.

Breakspear, M., Terry, J. R., and Friston, K. J. (2003) Modulation of excitatory synaptic coupling facilitates synchronization and complex dynamics in a biophysical model of neuronal dynamics. Network 14, 703–732.

Chartrand, G. and Lesniak, L. (1996) *Graphs and Digraphs*. Chapman and Hall, Boca Raton, FL.

Cocomac (2003) Collations of Connectivity Data on the Macaque Brain. http://www.cocomac.org.

Crick, F. and Jones, E. (1993) The backwardness of human neuroanatomy. Nature 361, 109–110.

Felleman, D. J. and Van Essen, D. C. (1991) Distributed hierarchical processing in the primate cerebral cortex. Cerebral Cortex 1, 1–47.

Graziano, M. S. A, Reiss, L. A. J., and Gross, C. D. (1999) A neuronal representation of the location of nearby sounds. Nature 397, 428–430.

Harary, F. (1969) *Graph Theory*. Addison-Wesley, Reading, MA.

Hellwig, B. (2000) A quantitative analysis of the local connectivity between pyramidal neurons in layers 2/3 of the rat visual cortex. Biol. Cybern. 82, 111–121.

Hilgetag, C. C., Burns, G. A. P. C., O'Neill, M. A., Scannell, J. W., and Young, M. P. (2000) Anatomical connectivity defines the organization of clusters of cortical areas in the macaque monkey and the cat. Philosophical Transactions of the Royal Society London B 355, 91–110.

Jeong, H., Tombor, B., Albert, R., Oltvai, Z. N. and Barabasi, A. -L. (2000) The large-scale organization of metabolic networks. Nature 407, 651–654.

Kleinberg, J. M. (2000) Navigation in a small world. Nature 406, 845.

Kötter, R. (2001) Neuroscience databases: tools for exploring brain structure-function relationships. Philosophical Transactions of the Royal Society London B 356, 1111–1120.

Kötter, R. and Stephan, K. E. (2003) Network participation indices: Characterizing component roles for information processing in neural networks. Neural Networks, 16, 1261–1275.

Latora, V. and Marchiori, M. (2001) Efficient behavior of small-world networks. Phys. Rev. Lett. 87, #198701.

Lewis, J. W. and Van Essen, D. C. (2000) Cortico-cortical connections of visual, sensorimotor, and multimodal processing areas in the parietal lobe of the Macaque monkey. J. Comp. Neurol. 428, 112–137.

Liley, D. T. J. and Wright, J. J. (1994) Intracortical connectivity of pyramidal and stellate cells: estimates of synaptic densities and coupling symmetry. Network: Computation in Neural Systems 5, 175–189.

Martin, R., Kaiser, M., Andras, P., and Young, M. (2001) Is the brain a scale-free network? Soc. Neurosci. Abstr. 27, 814–816

Maslov, S. and Sneppen, K. (2002) Specificity and stability in topology of protein networks. Science 296, 910–913.

Milgram, S. (1967) The small world problem. Psychol. Today 1, 61–67.

Milo, R., Shen-Orr, S., Itzkovitz, S., Kashtan, N., Chklovskii, D., and Alon, U. (2002) Network motifs: simple building blocks of complex networks. Science 298, 824–827.

Nicoll, A. and Blakemore, C. (1993) Patterns of local connectivity in the neocortex. Neural Computation 5, 665–680.

Passingham, R. E., Stephan, K. E., and Kotter, R. (2002) The anatomical basis of functional localization in the cortex. Nature Reviews Neuroscience 3, 606–616.

Ravasz, E., Somera, A. L., Mongru, D. A., Oltvai, Z. N., and Barabasi, A. -L. (2002) Hierarchical organization of modularity in metabolic networks. Science 297, 1551–1555.

Rives, A. W. and Galitski, T. (2003) Modular organization of cellular networks. Proc. Natl. Acad. Sci. USA 100, 1128–1133.

Scannell, J. W. and Young, M. P. (1993) The connectional organization of neural systems in the cat cerebral cortex. Current Biology 3, 191–200.

Scannell, J. W., Blakemore, C., and Young, M. P. (1995) Analysis of connectivity in the cat cerebral cortex. Journal of Neuroscience 15, 1463–1483.

Scannell, J. W., Burns, G. A. P. C., Hilgetag, C. C., O'Neil, M. A., and Young, M. P. (1999) The connectional organization of the cortico-thalamic system of the cat. Cerebral Cortex 9, 277–299.

Sporns, O. (2002) Graph theory methods for the analysis of neural connectivity patterns. Kötter, R. (ed.) *Neuroscience Databases. A Practical Guide*, Klüwer, Boston, MA, pp. 171–185.

Sporns, O. (2004) Complex neural dynamics. In: Coordination Dynamics: Issues and Trends, Jirsa, V. K. and Kelso, J. A. S., eds. pp. 197–215.

Sporns, O., Tononi, G., and Edelman, G. M. (2000) Theoretical neuroanatomy: Relating anatomical and functional connectivity in graphs and cortical connection matrices. Cerebral Cortex 10, 127–141.

Sporns, O. and Tononi, G. (2002) Classes of network connectivity and dynamics. Complexity 7, 28–38.

Strogatz, S. H. (2001) Exploring complex networks. Nature (London) 410, 268–277.

Tononi, G., Edelman, G. M., and Sporns, O. (1998) Complexity and coherency: Integrating information in the brain. Trends in Cognitive Sciences 2, 474–484.

USC Brain Project (2003) http://www-hbp.usc.edu/.

Varela, F., Lachaux, J. -P., Rodriguez, E., and Martinerie, J. (2001) The brainweb: phase synchronization and large-scale integration. Nature Reviews Neuroscience 2, 229–239.

Watts, D. J. and Strogatz, S. H. (1998) Collective dynamics of 'small-world' networks. Nature 393, 440–442.

Watts, D. J. (1999) *Small Worlds*. Princeton University Press, Princeton, NJ.

Watts, D. J. (2003) *Six Degrees. The Science of a Connected Age*. W.W. Norton, New York.

Young, M. P. (1993) The organization of neural systems in the primate cerebral cortex. Proc. R. Soc. Lond. B 252, 13–18.